Constraints on Thermal Evolution of Asteroid Fragments from High Temperature Cooling Rates. Jialong Ren[1], Marc A. Hesse[1], Michael P. Lucas[2] and Nick Dygert[3], [1]Department of Geological Sciences, University of Texas at Austin (jialongren@utexas.edu), [2]Department of Civil and Environmental Engineering and Earth Sciences, University of Notre Dame, [3]Department of Earth & Planetary Sciences, University of Tennessee, Knoxville.

Introduction: Application of REE-in-two-pyroxene thermometry, two-pyroxene solvus thermometry and Ca-in-olivine thermometry to meteorites from H, L, LL chondrite and acapulcoite-lodranite parent bodies reveals fast (~1 °C/y) cooling from peak or near-peak temperatures (temperature denoted as T below) [1,2]. Our previous work [1,3] shows that fast cooling at high T can be reconciled with the two-six orders of magnitude slower cooling at low T e.g., [4,5] by fragmentation -reassembly events [1,6,7], where the parent asteroids were collisionally disrupted at peak or near-peak T. After fragments reassemble into a rubble pile, they stop being exposed to space and continue to cool more slowly.

During the disruption of the body the fragments cool by conduction as they are exposed to ambient T. The conductive cooling rate declines with time, so that the observed high-T cooling rate provides information on the cooling time and the fragment size. To obtain quantitative constraints we need to understand the cooling rate at the closure T of the geothermometer. Therefore, we develop analytic models for the decline of the cooling rate at fixed T.

Models: For simplicity, we consider the conductive cooling of a sphere with radius R and constant properties including porosity φ, non-porous grain density grain density ρ, specific heat capacity c_p and thermal conductivity k_φ. A uniform initial T is also assumed for any individual fragment which is exposed to a lower ambient T. The T rise from the decay of ^{26}Al at potential fragmentation time is 2 to 5 orders of magnitude lower than the high T cooling rate [1], so that we neglect radiogenic heating. The analytic solution of this 1-D problem is given by an error-function-series solution [8]. The T and cooling rate at different times for a 10 km-radius H chondrite fragment is shown in Fig. 1. The properties [9] are φ=0.1 , ρ=3720 kg/m^3, c_p=837 J/kg/K and k_φ=1.23 W/m/K, so that the diffusivity =4.410^{-7} m^2/s. To compare with cooling rate data, we need to extract the cooling rate at the closure T of the geothermometer from the analytical solution.

When the cooling time is much shorter than the diffusion time scale, the spherical solution is approximate to a semi-infinite planar solution. In the planar solution, the T profile is self-similar in the Boltzmann variable $\eta = x/2\sqrt{\kappa t}$. Conversely, η is a constant for a given T, which shows that the cooling rate at a given T declines proportional to 1/t.

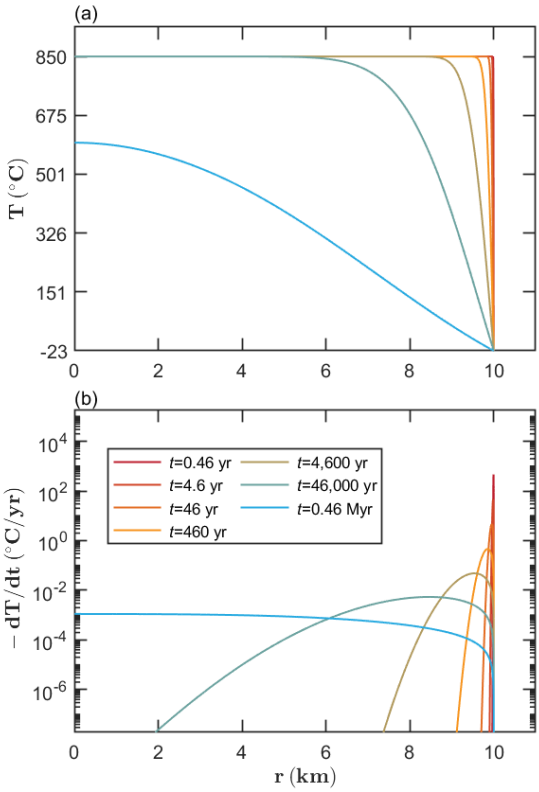

Figure 1.(Modified from Fig. 2 in [9]) Conductive cooling of a 10 km-radius H chondrite spherical fragment: (a) Radial T profiles at increasing times, for legend see panel b. (b) Radial cooling rate profiles at increasing times.

Result: Cooling rates though 700 °C of five H chondrite fragments with different radii are shown in Fig. 2a. The black dash line refers to the semi-infinite planar cooling, which provides a lower boundary for the spherical solution. The spherical cooling rates initially follow decay of the planar solution. Then they curve upward when the cooling reaches the center of the fragments. This deviation occurs later in larger fragments. Once the center reaches 700 °C, the cooling at this T ends as a dot in Fig. 2a. Those dots together provide an upper boundary (solid black line) of the cooling rate as a function of t at a given T that also follows the 1/t decline.

For H chondrite data [1], the high T cooling rate ranges from 10^{-2} to 10 °C/yr. This suggests that

minimum cooling times from 18.7 to 18,700 years are required to attain such cooling rates. It is also worth noting that lines for smaller fragments in Fig. 2a end before the 10^{-2} °C/yr rate occurs. Therefore, the cooling rate data also place a constraint on the radius of the spherical fragment, as shown in Fig. 2b. The minimum fragment radius is proportional to $1/\sqrt{-\,dT/dt}$.

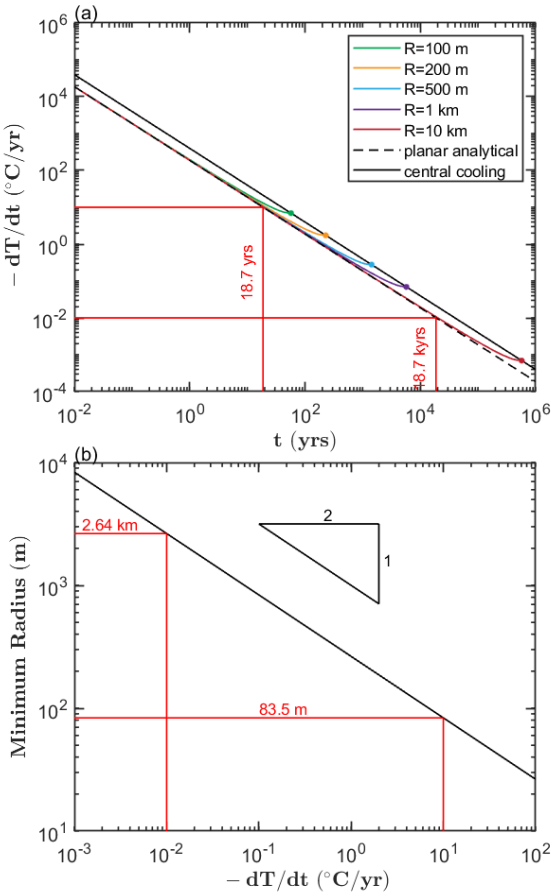

Figure 2. (Modified from Fig. 3 in [9]) Cooling rates at 700 °C as functions of time (log-log scale) for spherical H chondrite fragments with different radii. Red lines show the minimum cooling times for the cooling rates observed in H chondrites. (b) Minimum radii as a function of cooling rate at 700 °C . Red lines show the minimum fragment radii required to attain the cooling rates observed in H chondrites. The triangle indicates the slope in this logarithm scale.

In Fig. 3 cooling rates are plotted against T and compared with data from multiple geothermometers. Black lines show the path of different shells within the fragment and colorful lines show the state at a given time. There is a plateau of cooling rates in the medium T range at any given time. At 0.46 Myrs the center has already cooled to about 600 °C, so that the blue line does not begin from the initial T.

Discussion: Comparison with the data shows that the simple conductive cooling model can produce the observed fast cooling at high T. However, it is difficult to model the cooling path through multiple cooling rates at different T. Both REE and the Ca-Ol data have been measured in the same samples so that a single black line should connect both pairs of data. The conductive model generally predicts a slower decline of the cooling rate with T.

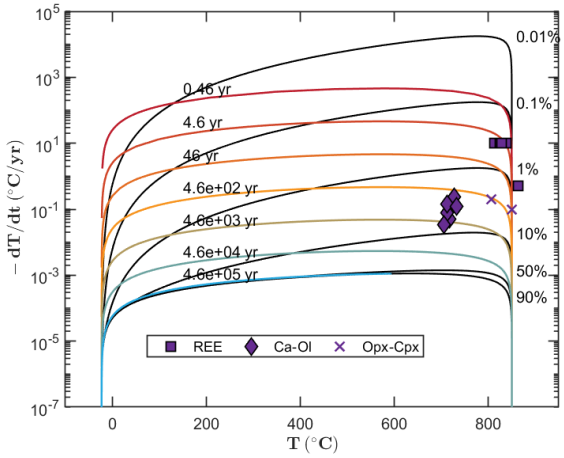

Figure 3. Cooling rates as functions of T for different radii (black lines, depth in the indicated right of the lines) and at different times in colorful lines of a 10 km-radius H chondrite fragment. Cooling rates are compared with H chondrite data [1].

The model provides lower bounds of cooling time (Fig. 2a) that exceed the reassembly time of hours to years commonly suggested by dynamical arguments e.g., [10]. It may therefore be necessary to consider more realistic assumptions to bridge this discrepancy. A more appropriate boundary condition is the radiation boundary. If we consider fragments radiating to hot dust, it will effectively increase the surface T in the current case and shorten the minimum cooling time by shifting lines in Fig. 3a downward. The effect of impact heating and multi-stage reassembly are also interesting to consider in the future steps.

Acknowledgments: This work was funded by NASA-SSW grant #80NSSC19K0030.

References: [1] Lucas M. P. et al. (2020) *GCA, 290,* 366–390. [2] Lucas et al., submitted to *Meteoritics & Planet. Sci.*. [3] Ren J. et al. (2021) *LPSC LII,* Abstract #2620. [4] Scott E.R.D. (2002) *Asteroids III,* 697-709. [5] Pellas P. and Storzer D. (1981) *PRSL 374*, 253-270. [6] Grimm, R.E. (1985) *JGR 90*, 2022-2028. [7] Blackburn, T.et al. (2017) *GCA, 200*, 201-217. [8] Crank, J. (1975) The mathematics of diffusion, 2nd edn. [9] Jialong et al., submitted to *Icarus*. [10] Love, S.G. and Ahrens, T.J. (1996) *Icarus 124*, 141-155.